OAK RIDGE NATIONAL LABORATORY
OPERATED BY
UNION CARBIDE CORPORATION
NUCLEAR DIVISION
POST OFFICE BOX X
OAK RIDGE, TENNESSEE 37830

ORNL/MIT-221

DATE: December 17, 1975 COPY NO.

SUBJECT: Determination and Correlation of Mass Transfer Coefficients in a Stirred Cell

Authors: J. Herranz, S.R. Bloxom, J.B. Keeler, and S.R. Roth

Consultants: C.H. Brown and J.R. Hightower

ABSTRACT

In the proposed Molten Salt Breeder Reactor flowsheet, a fraction of the rare earth fission products is removed from the fuel salt in mass transfer cells. To obtain design parameters for this extraction, the effect of cell size, blade diameter, phase volume, and agitation rate on the mass transfer for a high density ratio system (mercury-water) in non-dispersing square cross section contactors was determined. Aqueous side mass transfer coefficients were measured by polarography over a wide range of operating conditions. Correlations for the experimental mass transfer coefficients as functions of the operating parameters are presented. Several techniques for measuring mercury-side mass transfer coefficients were evaluated, and a new one is recommended.

RSA

Oak Ridge Station
School of Chemical Engineering Practice
Massachusetts Institute of Technology

Contents

1. SUMMARY

Film mass transfer coefficients were determined in stirred, square cells with large density difference liquids. The effects of cell size, phase height, blade length, and stirring speed were evaluated. There was no significant dependence on the ratio of blade length to cell length or phase height; however, a strong relationship of mass transfer coefficient with blade length and stirring speed was noted. The power law correlation was

$$\frac{KL}{\nu_m} = 2.58 \times 10^{-5} \, Re_m^{1.169 \pm 0.030}$$

The object of this investigation was to determine and to correlate film mass transfer coefficients for design of the fuel salt processing section in the Molten Salt Breeder Reactor. In this process, molten fuel salt containing rare earth metal fluorides is contacted with liquid bismuth containing lithium as a reductant. The contactors will be square graphite vessels with agitators in each phase. The correlation of mass transfer coefficient for high density non-dispersing systems is necessary to size this process.

The experimental system consisted of various size square Plexiglas cells with a dense mercury phase and a light aqueous phase. Agitation was provided by paddles of several lengths centered in each phase. The mass transfer rate of quinone was measured by polarography with the mercury phase as the polarized cathode and a gold or silver anode suspended in the aqueous phase. The concentration of hydroquinone was 50 times that of quinone to prevent anode polarization. Both concentrations remain constant since oxidation and reduction occur simultaneously and stoichiometrically.

An established technique for mercury side mass transfer determination did not exist. The feasibility of a proposed method was determined. In this method, an oxidizing agent in the aqueous phase oxidizes a metal amalgamated with the mercury. The progress of this reaction is monitored by the potential of the redox couple against a standard calomel electrode. Ferric ion was not suitable as an oxidizing agent because it also oxidized the mercury. The oxidation of zinc by hydrochloric acid also failed because the rate of reaction was too slow. The general method still deserves further development.

2. INTRODUCTION

2.1 Background

A breeder reactor produces more fissionable material than it consumes; in addition, protactinium and rare earth byproducts are created. In the Molten Salt Breeder Reactor (MSBR) these excess fission products leave the reactor in the fuel salt stream. Removal of protactinium and rare earth fission products from the fuel salt stream of a MSBR is a critical step in the proposed processing scheme. To achieve good breeding in a MSBR, some of the salt-soluble fission products, and particularly the rare earths, must be removed rapidly. A flowsheet of the proposed processing scheme is shown in Fig. 1.

In the fluorinator, uranium is volatilized from the molten salt as uranium hexafluoride by contacting it with fluorine. The reductive extraction process contacts liquid bismuth containing dissolved lithium with the fuel salt stream to extract the protactinium and to transfer it to another salt stream. Here, the protactinium remains in solution until it decays naturally to uranium which is volatilized with fluorine. The uranium- and protactinium-free salt stream is then contacted again with the bismuth-lithium amalgam, extracting the remaining rare earth fission products. These rare earths are then re-extracted into lithium chloride and finally selectively extracted from the lithium chloride for storage and disposal. The uranium hexafluoride is injected into the purified salt stream and returned to the reactor.

The protactinium is removed by reductive extraction with lithium. The lithium is oxidized to Li^{+1} entering the salt phase as lithium fluoride. The protactinium is reduced from protactinium tetrafluoride to metallic protactinium and dissolved in the bismuth phase. This contacting must take place without entrainment of bismuth in the salt phase as bismuth is corrosive to the reactor containment alloy. Hence a contactor which maximizes mass transfer while minimizing entrainment is desirable.

2.2 Previous Work

Lewis (3) investigated mass transfer rates in cylindrical, non-dispersed, two-phase, mechanically-agitated cells, with several aqueous-organic systems. He correlated his results by an empirical equation,

$$\frac{60\ K_1}{\nu_1} = 6.76 \times 10^{-6} \left(Re_1 + Re_2 \frac{\eta_2}{\eta_1}\right)^{1.65} + 1 \qquad (1)$$

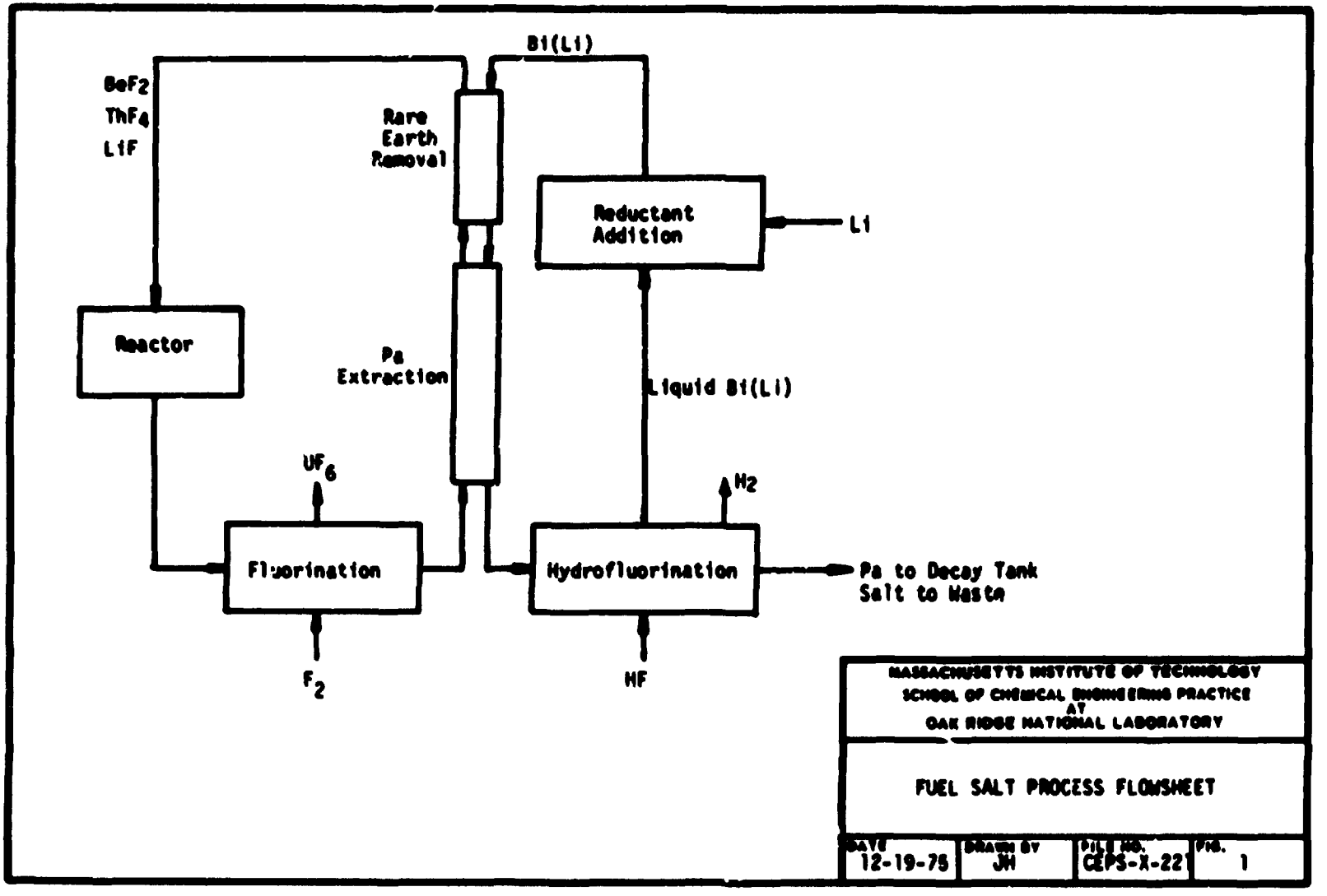
Bi(Li)
BeF2
ThF4
LiF
Rare Earth Removal
Reductant Addition
Li
Reactor
Pa Extraction
Liquid Bi(Li)
UF6
H2
Fluorination
Hydrofluorination
Pa to Decay Tank
Salt to Waste
F2
HF
MASSACHUSETTS INSTITUTE OF TECHNOLOGY
SCHOOL OF CHEMICAL ENGINEERING PRACTICE
AT
OAK RIDGE NATIONAL LABORATORY
FUEL SALT PROCESS FLOWSHEET
DATE
12-19-75
DRAWN BY
JH
FILE NO.
CEPS-X-221
FIG.
1

When stirrer speeds and stirrer lengths are equal in both phases, the above equation can be reduced to the form

$$\frac{60\ K_1}{v_1} = 6.76 \times 10^{-6} \left[Re_1\left(1 + \frac{\rho_2}{\rho_1}\right)\right]^{1.65} + 1 \qquad (2)$$

Lewis postulated that mass transfer was only a function of eddy transport to and from the interface and was independent of the molecular diffusivity of the observed systems over the range of Reynolds numbers considered. The range of liquid densities varied from 0.8 to 1.2 g/cm^3. McManamey (5) correlated his own data and Lewis' results by the following expression:

$$\frac{60\ K_1}{v_1} = 0.102\ (Re_1)^{0.9}\left(1 + \frac{Re_2}{Re_1}\frac{\eta_2}{\eta_1}\right)(Sc_1)^{-0.37} \qquad (3)$$

which is similar to that by Lewis but includes the Schmidt number. For equal stirrer speeds and lengths in each phase this reduces to:

$$\frac{60\ K_1}{v_1} = 0.102\ (Re_1)^{0.9}\left(1 + \frac{\rho_1}{\rho_2}\right)(Sc_1)^{-0.37} \qquad (4)$$

Mayers (4) developed an improved correlation on the basis of Lewis' data and confirmed it by additional experimental data on new systems:

$$\frac{K_1 L}{D_1} = 0.00316(Re_1 Re_2)^{1/2}\left(\frac{\eta_2}{\eta_1}\right)^{1.9}\left(0.6 + \frac{\eta_2}{\eta_1}\right)^{-2.4}(Sc_1)^{5/6} \qquad (5)$$

This equation reduces to Eq. (6) when stirrer speeds and lengths are equal.

$$\frac{K_1 L_1}{D_1} = 0.00316(Re_1)\left(\frac{\eta_2}{\eta_1}\right)^{1.4}\left(0.6 + \frac{\eta_2}{\eta_1}\right)^{-2.4}\left(\frac{\rho_2}{\rho_1}\right)^{0.5}(Sc_1)^{5/6} \qquad (6)$$

The effect of the molecular diffusion coefficient, D, on the film coefficient of mass transfer is not entirely negligible for the stirred cell system, so that the transfer is not completely controlled by eddy diffusivity. It was found that K_1 is proportional to $D_1^{1/6}$. This is less than the exponent of 1/2 expected for unsteady state diffusion to a

stagnant surface (unstirred system) and approaches the exponent of zero expected if the transfer takes place by a turbulent mixing process. In practice, for well-stirred conditions and in the presence of clean liquid-liquid interfaces, the exponent will lie between 0.5 and 0.0 since the physical process involves both penetration and turbulent mixing at the interface. All the above equations correlate the data for systems of similar density liquids well; the Mayers and McManamey correlations provide a slightly better fit than the Lewis correlation.

Hightower (2) presented the following correlation to fit the experimental results in a water-mercury system:

$$\frac{60\,K_1 L}{\nu_1} = 0.2058(Re_1)\left(\frac{\eta_2}{\eta_1}\right)^{1.4}\left(0.6 + \frac{\eta_2}{\eta_1}\right)^{-2.4}(Sc_1)^{-1/6}\left(\frac{\rho_2}{\rho_1}\right)^{0.27}\left(\frac{L}{H}\right)^{0.45} \quad (7)$$

This correlation was obtained using the Mayers correlation as the best of the existing correlations and adding two additional terms to include the effect of the density ratio of the two phases (ρ_1/ρ_2) and a geometrical ratio, L/H, where H is the height of an individual phase and L is the tip-to-tip impeller length.

Predictions from different correlations were compared with experimental results from experiments conducted in a 7-3/4 x 10-1/2-in. contactor with a 5000-cc volume for each phase. While the Lewis correlation vastly overpredicts the mass transfer coefficients, the modified correlation usually underpredicts them, although to a somewhat lesser degree. The modified correlation predicts the aqueous-organic systems as accurately as the Mayers correlation and fits the experimental water-mercury data with a standard deviation of 25% (2). These results indicate that the mass transfer rates in the salt-bismuth system fall between the Lewis correlation and the modified correlation [Eq. (7)] obtained at ORNL.

Note that all the investigators have found a different dependence on the molecular diffusivity. In addition, most of the previous experiments have been performed in cylindrical cells with liquids of nearly equal densities and mass transfer results were based on measurements of bulk phase concentration. Therefore, no distinction can be made between mass transfer at the bulk phase boundary between two liquids and at the phase boundaries of entrained material.

If dispersion occurred in any of the experiments, the value of apparent diffusional mass transfer coefficient would be enhanced and the dependence on molecular diffusivity coefficient would be larger. Hence, the previous correlations may not be directly applicable to the design of the proposed bismuth-fuel salt contactor which is a graphite vessel of square cross section with a bismuth/fuel salt density ratio of about three.

2.3 Objectives and Method of Attack

The objective is to determine the effect of cell and paddle sizes, stirring speed, and phase volume on the water side mass transfer coefficient in a stirred cell containing water and mercury. Dimensional analysis of the results will determine important dimensionless groups by regression analysis. In addition, the feasibility and possible development of a proposed experiment for measuring mercury side mass transfer coefficients will be determined by running the experiment with certain specific materials while seeking possible alternative materials consistent with the general procedure and theory.

3. THEORY

3.1 Polarographic Determination of Mass Transfer Coefficients

The polarographic technique for determining mass transfer coefficients involves oxidation of a reduced species or reduction of an oxidized species at an electrode which is at a condition of concentration polarization. Polarization of the cathode can be accomplished in one of two ways: either the anode surface area is made very large with respect to the cathode surface area, or the concentration of the oxidized species is made very small with respect to the reduced species.

The migration of an ion in combined electric and concentration fields is described by the Nernst-Planck equation:

$$J = D\left(\frac{\partial C}{\partial r} + ZuCF\,\frac{\partial \phi}{\partial r}\right) \qquad (8)$$

where the first term on the righthand side represents the contribution of ordinary diffusion to the flux, and the second term represents the contribution of electromigration. When the concentration of an inert electrolyte (relative to that of the reacting ion) is large, the dielectric properties of the solution are altered such that the potential will decrease smoothly across the region between the electrodes while the reacting ion concentration drops sharply across the thin, polarized layer near the cathode. Thus, the term containing the electric potential becomes relatively small, and Eq. (8) can be expressed as,

$$J \cong D\,\frac{\partial C}{\partial r} \qquad (9)$$

Then the current flowing between the electrodes is a measure of mass transfer rates governed by ordinary molecular diffusion. This current is sometimes called the diffusion current.

The total molar flow rate of ions at the interface is described by the product of a concentration driving force, the interfacial area for mass transfer, and the mass transfer coefficient:

$$Q = KA(C_b - C_i) \tag{10}$$

Rearranging, the mass transfer coefficient is given by,

$$K = \frac{Q}{A(C_b - C_i)} \tag{11}$$

The molar flow is related to the current measured across the cell by the equation

$$Q = \frac{I}{ZF} \tag{12}$$

If Eq. (12) is substituted into Eq. (11), the mass transfer coefficient across the stagnant layer between the bulk electrolyte and the polarized cathode is obtained as a function of the current through the contactor cell:

$$K = \frac{I}{(Z)(F)(A)(C_b)} \tag{13}$$

assuming that $C_i << C_b$.

3.2 Determination of Mercury-Side Mass Transfer Coefficients

The proposed experiment calls for dissolving a metal in mercury, then extracting the metal by contacting the mercury with an aqueous solution containing an excess of oxidizing agent. This excess insures the mass transfer limitation will be on the mercury side. The equation for the molar flow rate of metal is:

$$Q = KA(C_{b,m} - C_{i,m}) \tag{10}$$

or

$$Q = -V_m \frac{dC_{b,m}}{dt} \tag{14}$$

When one equates the flow rates,

$$-V_m \frac{dC_{b,m}}{dt} = KA(C_{b,m} - C_{i,m})$$

assumes $C_i = 0$,

$$\frac{dC}{C} = -\frac{KA}{V} dt$$

and integrates, ore obtains the expression

$$\ln \frac{Ct_2}{Ct_1} = -\frac{KA}{V}(t_2 - t_1) \tag{15}$$

for determining the mass transfer coefficient. By plotting the natural logarithm of the concentration ratio against elapsed time, the mass transfer coefficient can be found from the slope.

The concentration of metal will be monitored by the cell potential of the oxidizing agent in its oxidized and reduced forms against a standard calomel electrode. The Nernst equation

$$E = E^\circ + \frac{RT}{nF} \ln \frac{(OA^{ox})}{(OA^{red})} \tag{16}$$

relates this potential to the ratio of the concentration of the two forms. This information along with a mass balance on the oxidizing agent determines the concentration of the reduced form. This is stoichiometrically related to the amount of metal that has been oxidized.

Certain requirements must be met in the selection of metals and oxidizing agents. The metal must form an amalgam with mercury so that it can be extracted and must also be more easily oxidized than mercury so that the mercury will not also react. In addition, the oxidized form of the metal must be soluble in water with the anion of the oxidizing agent. Finally, the metal should only be capable of reducing the oxidizing agent

once. Further reduction would at least complicate and possibly render impossible the potentiometric monitoring of the concentration of redox couple.

The oxidizing agent must be compatible with the metal. It should oxidize the metal but not the mercury, and not be further reduced by the metal. It must also be soluble in aqueous solution in both oxidized and reduced forms.

4. APPARATUS AND PROCEDURE

4.1 Apparatus

4.1.1 Water Side Mass Transfer

Table 1 presents a summary of the experimental variables. A large

Table 1. Experimental Variables

Cell Size (in.)	Blade Size (in.)	Phase Volume (cm^3)	Agitator Speed Range (rpm)
4x4	2.5 x 0.75 3.5 x 0.75	700; 900	15 - 180
8x8	3.5 x 0.75 5.5 x 0.75 7.5 x 0.75	3000; 5000; 7000	15 - 140
12x12	3.5 x 0.75 5.5 x 0.75 7.5 x 0.75 9.5 x 0.75 11.0 x 0.75	9000; 18,000	15 - 65

number of experiments with various agitation rates were performed at each of the conditions listed in Table 1. Agitation rates were limited to values below the point at which dispersion of the phases became apparent. Dispersion could be detected by small droplets of water entering the mercury phase near the edge of the cell. The paddles in each phase were always identical in size and placed at equal distances from the interface. Figure 2 presents a detailed view of the general experimental cell and the potentiostat-recorder arrangement.

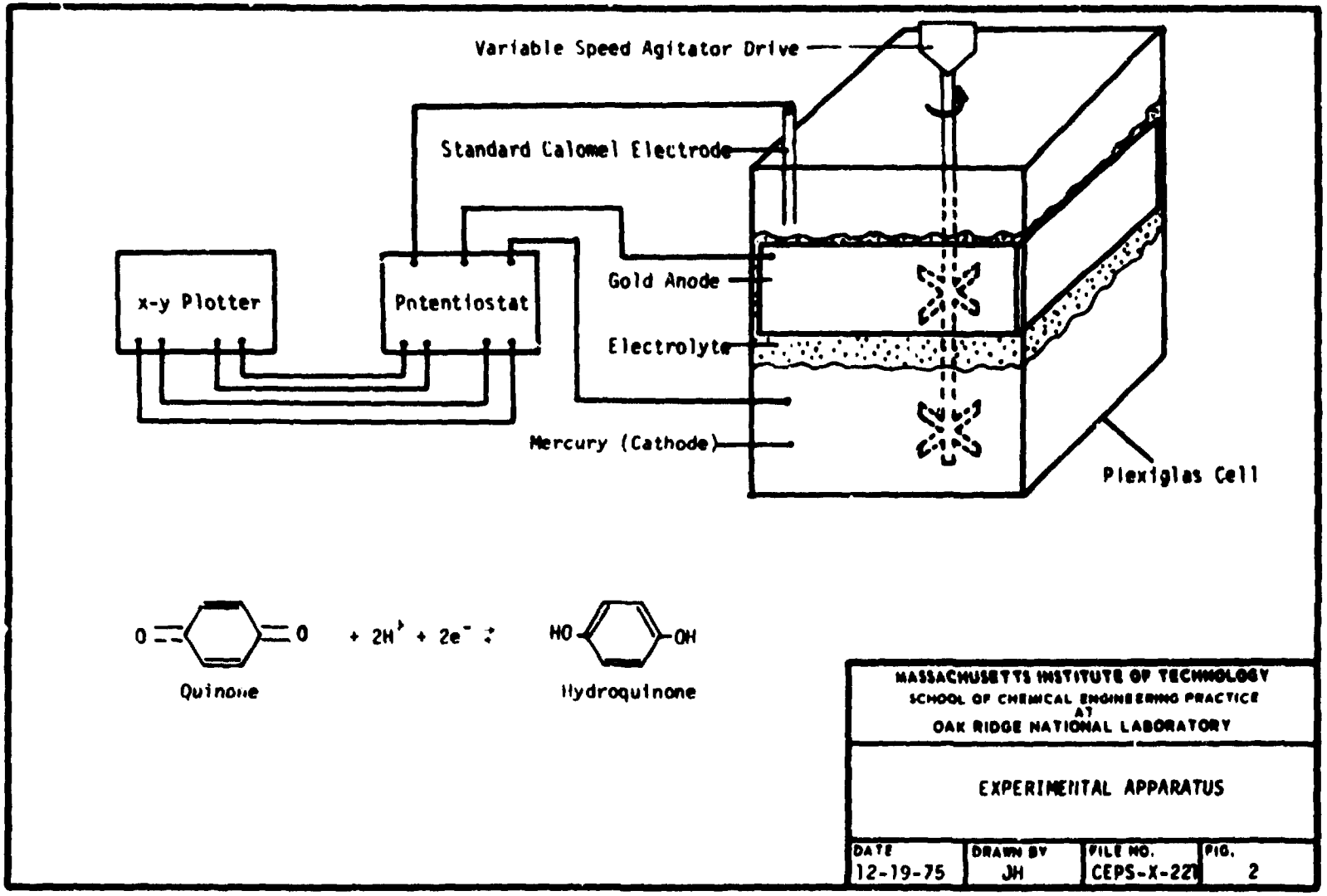
Variable Speed Agitator Drive
Standard Calomel Electrode
x-y Plotter
Potentiostat
Gold Anode
Electrolyte
Mercury (Cathode)
Plexiglas Cell
O
O
+ 2H⁺ + 2e⁻
HO
OH
Quinone
Hydroquinone
MASSACHUSETTS INSTITUTE OF TECHNOLOGY
SCHOOL OF CHEMICAL ENGINEERING PRACTICE
AT
OAK RIDGE NATIONAL LABORATORY
EXPERIMENTAL APPARATUS
DATE 12-19-75
DRAWN BY JH
FILE NO. CEPS-X-221
FIG. 2

The mercury surface in the electrochemical cell acted as the cathode. The potential of the mercury surface was measured against a standard calomel electrode in the aqueous phase. The anode of the cell was suspended in the aqueous electrolyte phase. In the 4x4-in. and 8x8-in. cells, the anode consisted of 0.0625-in. gold plating on 1/16-in. nickel sheet. In the 12x12-in. cell the anode was silver on nickel. All anodes fit closely inside the perimeter of the cell. The maximum current throughout the cell is inferred from the voltage drop across a 1.0-ohm (±0.5%) precision resistor. The voltage drop across the resistor (proportional to current) is recorded as the y-coordinate on a Hewlett-Packard x-y plotter. The x-coordinate on the plotter is produced by the voltage supplied to the cell which is a direct signal from the potentiostat. The electrolyte for the water-side mass transfer experiments in different contactors was a solution of quinone varying from 0.001 to 0.0002 M and hydroquinone from 0.05 to 0.01 M in a 0.2 M monobasic potassium phosphate buffer solution (pH ~ 7).

Shown in Fig. 3 are polarograms, measured with the electrolyte described above, in the 4x4-in. contactor with the 2.5x0.75-in. paddle and and with phase volumes of 0.900 liters at several agitation rates. The current through the cell is plotted as a function of the mercury surface potential relative to the standard calomel electrode (SCE). For a fixed value of agitation the current increases from zero at zero applied potential through a small maximum at about -0.5 v and becomes relatively constant at about -0.6 v. In the region of applied potential from -0.6 to -0.9 v, the current through the cell is relatively constant, limited by diffusion of quinone to the mercury surface where it is reduced. The diffusion current is related to the mass transfer coefficient through the electrolyte film by Eq. (13).

4.1.2 Mercury-Side Mass Transfer

The apparatus, shown in Fig. 4, consisted of a 150-ml beaker to hold the water and mercury phases, a platinum electrode and a standard calomel electrode for monitoring the cell potential, and a millivoltmeter for reading the potential when connected to the electrodes.

4.2 Procedure

4.2.1 Water-Side Mass Transfer

Monobasic potassium phosphate buffer solution (KH_2PO_4, 0.2 M, pH 7) was prepared with distilled water and was sparged continuously with argon to eliminate oxygen. The electrolyte solution was then prepared by first dissolving quinone in the buffer solution and subsequently hydroquinone to obtain the desired concentrations. The electrolyte was prepared in the dark and was continuously sparged with argon to avoid quinone decomposition or dissolution of oxygen.

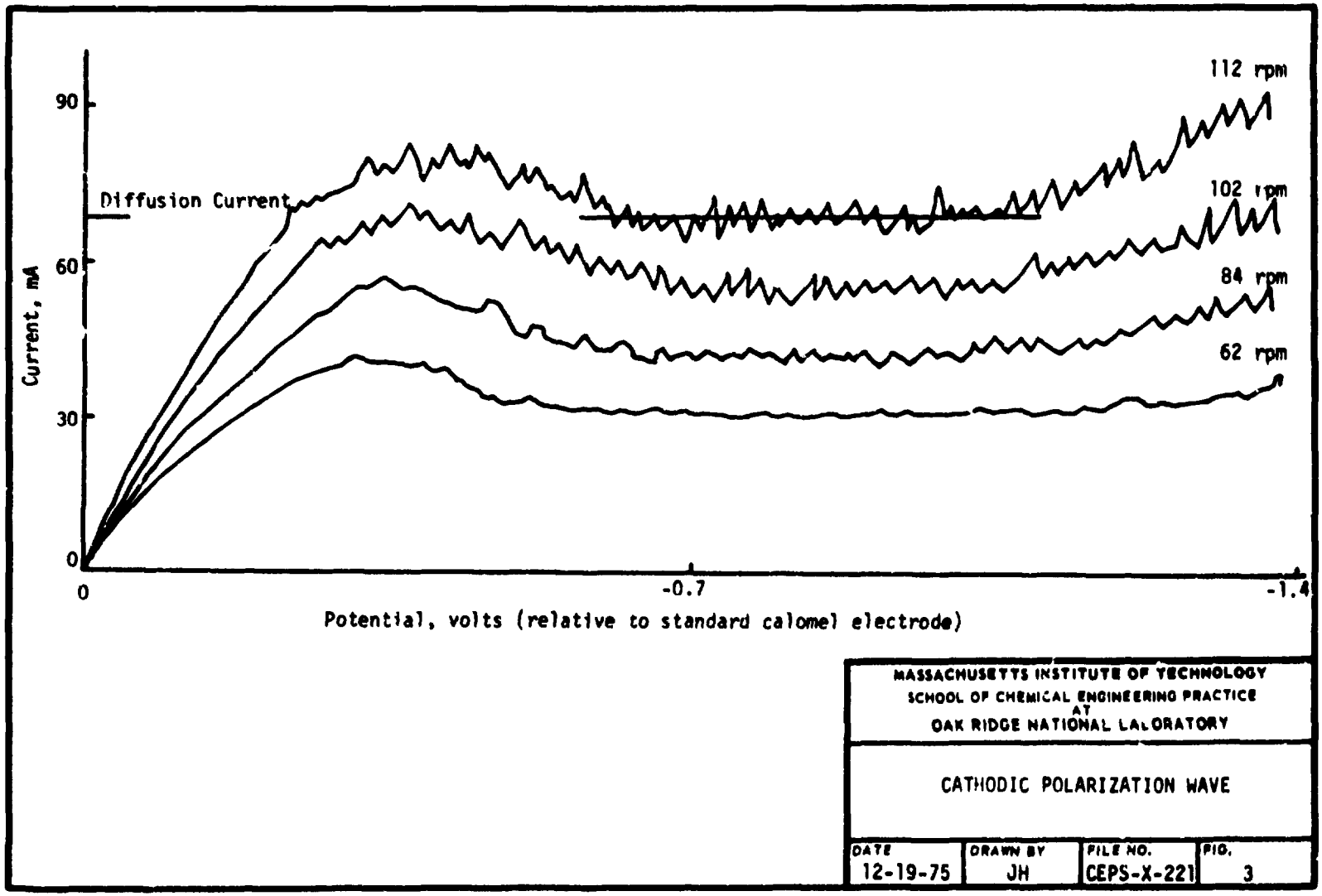
112 rpm
102 rpm
84 rpm
62 rpm
Diffusion Current
90
60
30
0
Current, mA
0
-0.7
-1.4
Potential, volts (relative to standard calomel electrode)
MASSACHUSETTS INSTITUTE OF TECHNOLOGY
SCHOOL OF CHEMICAL ENGINEERING PRACTICE
AT
OAK RIDGE NATIONAL LABORATORY
CATHODIC POLARIZATION WAVE
DATE 12-19-75
DRAWN BY JH
FILE NO. CEPS-X-221
FIG. 3

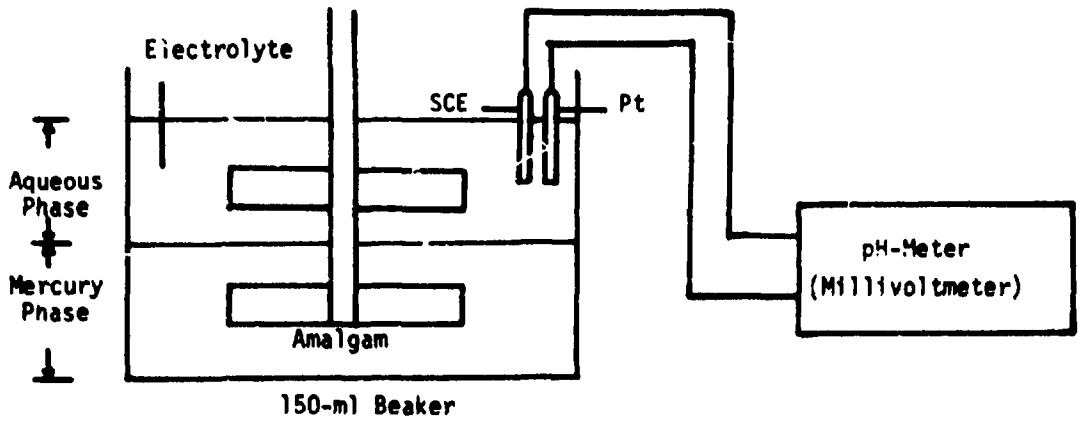

MASSACHUSETTS INSTITUTE OF TECHNOLOGY
SCHOOL OF CHEMICAL ENGINEERING PRACTICE
AT
OAK RIDGE NATIONAL LABORATORY

MERCURY-SIDE MASS TRANSFER APPARATUS

DATE	DRAWN BY	FILE NO.	FIG.
12-16-75	SR	CEPS-X-221	4

The required volume of mercury was measured into a graduated cylinder and added to the cell; then an equal volume of electrolyte solution was added. Phase heights were calculated and paddles located on the shaft such that they were centered in each phase, equidistant from the interface. The shaft was centered in the cell. The agitator speed was determined manually by counting the number of times an obstruction on the shaft hit one's finger in 30 sec. The speed was found to vary not more than 1 rpm.

Mass transfer coefficients were measured by the polarographic technique presented in Sect. 4.1.1.

4.2.2 Mercury-Side Mass Transfer

A known amount of lead was amalgamated with mercury. A solution of oxidizing agent (ferric chloride) of known concentration was prepared and the relative cell potential determined with a millivoltmeter, the other electrode being a platinum wire. The solution of oxidizing agent was added to a beaker containing the mercury amalgam and the voltage monitored as a function of time.

5. RESULTS AND DISCUSSION OF RESULTS

5.1 Water-Side Mass Transfer

5.1.1 Effect of Agitator Size on Mass Transfer Coefficient

As expected, the mass transfer coefficient is increased when blade diameter is increased for a particular cell size and agitator speed. This effect is shown in Fig. 5 for the 8x8-in. contactor with 5000 cm^3 phase volume and three different blades.

5.1.2 Effect of Phase Volume on Mass Transfer Coefficient

The effect of phase volume on the mass transfer coefficient was found to be slight as shown in Fig. 6 for the case of a 8x8-in. cell and 3.5 x 0.75-in. agitator.

5.1.3 Effect of Selective Phase Agitation on Mass Transfer Coefficient

At very low agitation rates when the mercury-water interface is not moving, the effect of agitation of the mercury phase was found negligible with respect to the agitation on the water phase. On the other hand, at higher agitation rates, agitation of the mercury phase is the only important parameter. The global performance is a result of a combination of agitation in both phases as shown in Fig. 7 for the 12x12 cell, 7.5x0.75-in. blade, and 18,000 cm^3 phase volume.

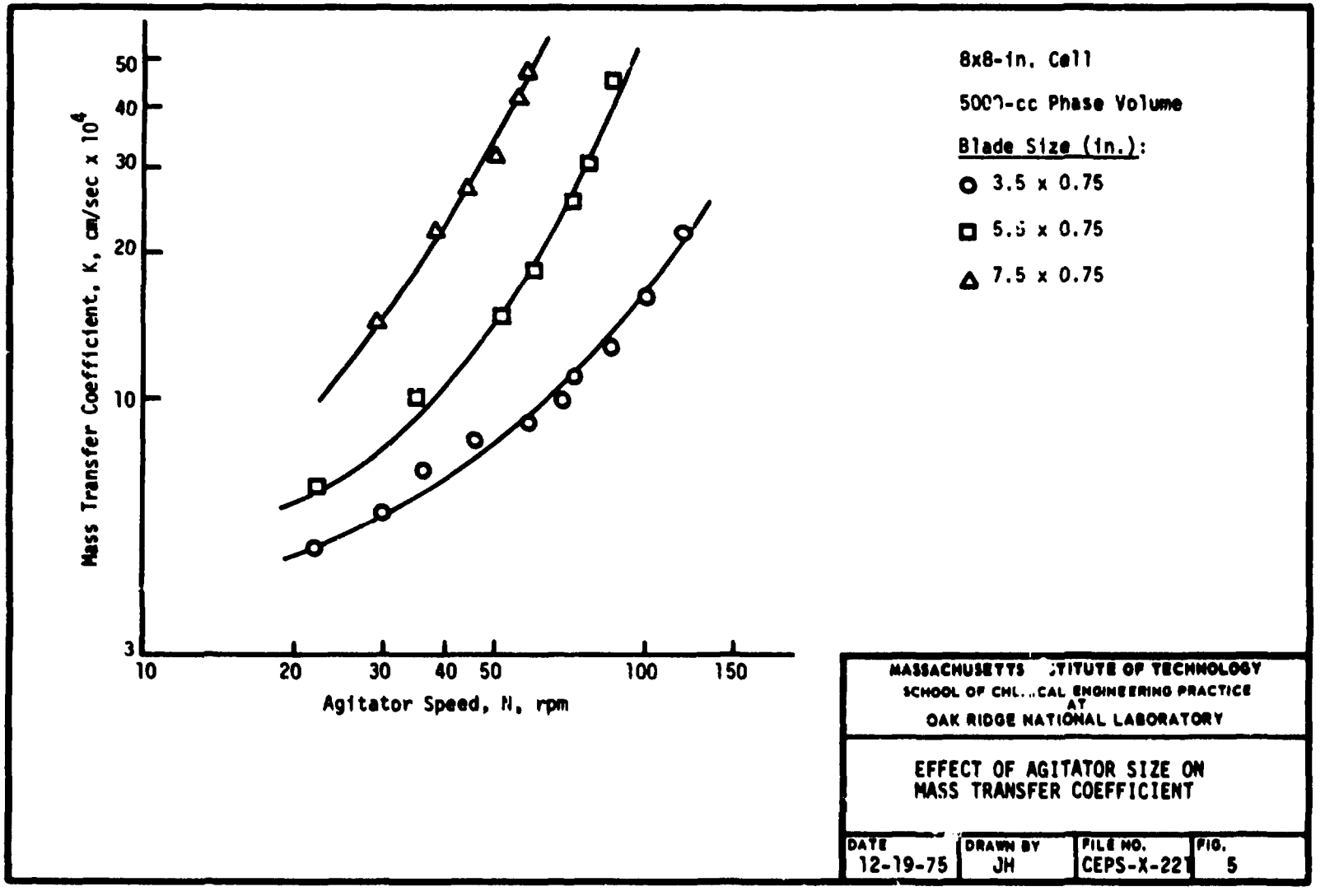
Mass Transfer Coefficient, K, cm/sec x 10^4
50
40
30
20
10
3
10
20
30
40
50
100
150
Agitator Speed, N, rpm
8x8-in. Cell
5000-cc Phase Volume
Blade Size (in.):
3.5 x 0.75
5.5 x 0.75
7.5 x 0.75
MASSACHUSETTS INSTITUTE OF TECHNOLOGY
SCHOOL OF CHEMICAL ENGINEERING PRACTICE
AT
OAK RIDGE NATIONAL LABORATORY
EFFECT OF AGITATOR SIZE ON
MASS TRANSFER COEFFICIENT
DATE 12-19-75
DRAWN BY JH
FILE NO. CEPS-X-221
FIG. 5

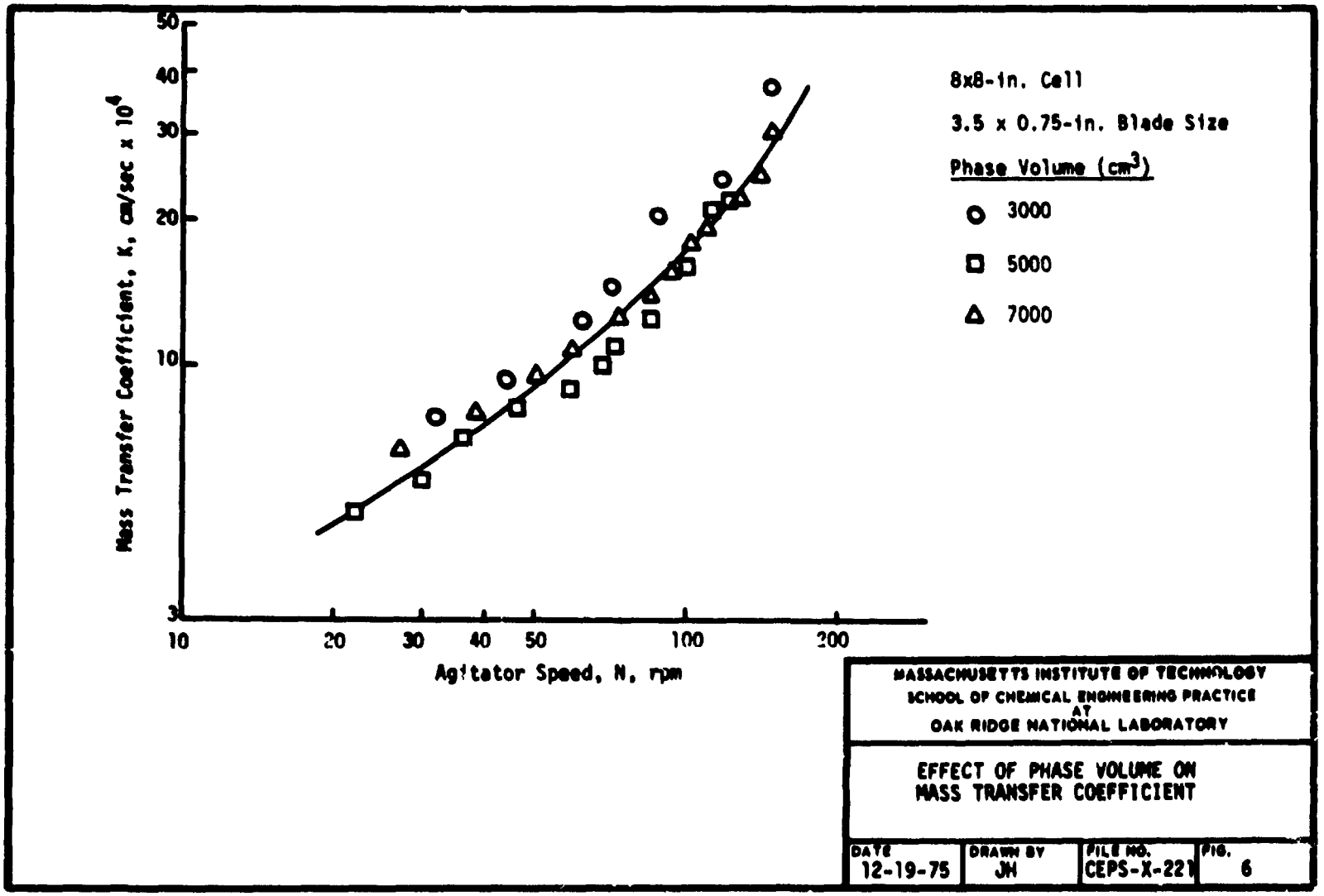
Mass Transfer Coefficient, K, cm/sec x 10^4
50
40
30
20
10
3
10
20
30
40
50
100
200
Agitator Speed, N, rpm
8x8-in. Cell
3.5 x 0.75-in. Blade Size
Phase Volume (cm^3)
3000
5000
7000
MASSACHUSETTS INSTITUTE OF TECHNOLOGY
SCHOOL OF CHEMICAL ENGINEERING PRACTICE
AT
OAK RIDGE NATIONAL LABORATORY
EFFECT OF PHASE VOLUME ON
MASS TRANSFER COEFFICIENT
DATE 12-19-75
DRAWN BY JH
FILE NO. CEPS-X-221
FIG. 6

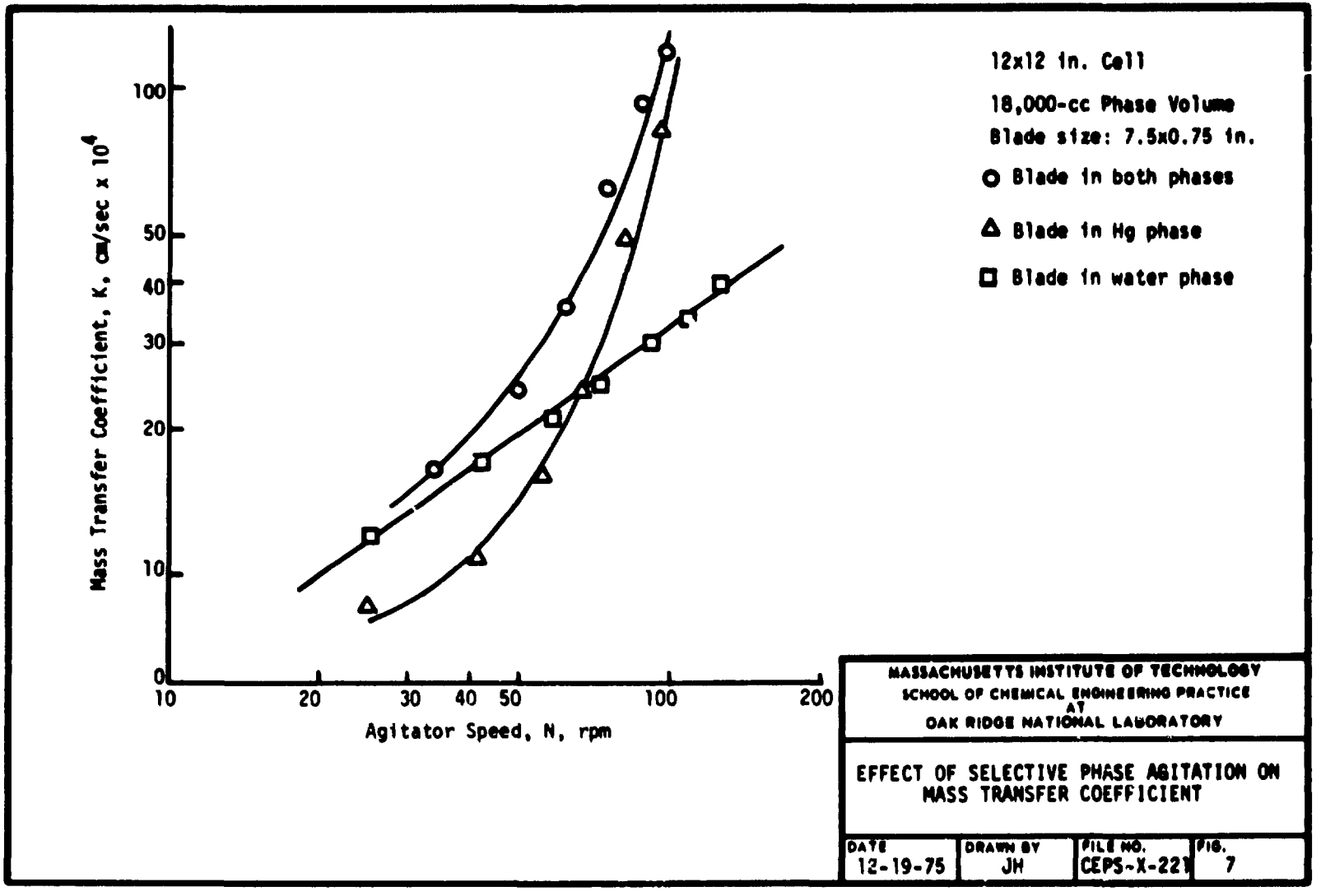
12x12 in. Cell
18,000-cc Phase Volume
Blade size: 7.5x0.75 in.
Blade in both phases
Blade in Hg phase
Blade in water phase
Mass Transfer Coefficient, K, cm/sec x 10^4
100
50
40
30
20
10
0
10
20
30
40
50
100
200
Agitator Speed, N, rpm
MASSACHUSETTS INSTITUTE OF TECHNOLOGY
SCHOOL OF CHEMICAL ENGINEERING PRACTICE
AT
OAK RIDGE NATIONAL LABORATORY
EFFECT OF SELECTIVE PHASE AGITATION ON MASS TRANSFER COEFFICIENT
DATE 12-19-75
DRAWN BY JH
FILE NO. CEPS-X-221
FIG. 7

5.2 Mercury-Side Mass Transfer

A 0.1-M ferric chloride solution (200 ml) was contacted with 50 ml of 0.05 M lead in mercury. The cell potential of the ferric-ferrous ion couple relative to a standard calomel electrode changed more rapidly than expected. A precipitate formed at the interface after about 1 min of reaction time. A precipitate due to the formation of plumbous chloride (solubility 1 g/100 ml of cold water) (1) was expected, but the amount formed was much larger than expected.

Due to the rapid potential change, indicating higher consumption of oxidizing agent than expected, and the quantity of precipitate formed, it was thought likely that the ferric chloride was oxidizing the mercury as well as the lead. To check this hypothesis some ferric chloride was added to clean mercury. Almost immediately a precipitate formed. Ferric chloride is therefore not a satisfactory oxidizing agent for metals amalgamated with mercury, due to its oxidation of the mercury itself. It may be possible to find a specific aqueous solution chemistry which will lower the potential of ferric ion relative to mercury sufficiently for its utilization. A preliminary review of the electromotive series did not reveal any such solution chemistry which is not reactive to mercury itself.

The possibility of using hydrochloric acid to oxidize zinc from mercury was also tested by monitoring pH to detect hydrogen ion consumption. Two experiments were run contacting 1.0 and 0.5 M hydrochloric acid with 0.05 and 1.0 M zinc in mercury, respectively. In each experiment, no significant change occurred in the pH during the course of the experiment. In addition, since this reaction liberates hydrogen, bubbles forming at the interface would be expected if the local hydrogen concentration exceeded its solubility; none were observed.

To check the concept of oxidizing zinc with hydrogen ion, another experiment was run in which 0.5 and 1.0 M HCl were brought into contact with zinc, no mercury present, and the pH observed. In this experiment, very gentle bubbling was observed, but again no change in pH occurred. The reaction of zinc with hydrochloric acid to form zinc chloride in aqueous solution is apparently so slow as to make changes in hydrogen ion concentration undetectable in time intervals of approximately one hour. Although the bubbling does indicate that the reaction is proceeding, the extremely slow evolution of gaseous hydrogen is further confirmation of the slow reaction rate. This slow rate makes mass transfer experiments impossible since the rate limiting step is the reaction rate, not the mass transfer rate.

Although neither of the above experiments were successful, the general technique remains promising. The savings in time and expense over other possible experimental methods (such as wet chemistry) still justify development of this general procedure. Other possible metals and oxidizing agents to investigate might include the stannic ion oxidation of lead with corresponding reduction to stannous ion. Possible health hazards exist with

powdered, tin salts however, so thorough precautions would be necessary. The oxidation of a more reactive metal with either hydrochloric acid or just water should be investigated.

5.3 Correlations

The mass transfer coefficient of quinone in water in a stirred cell was correlated with the cell operating parameters. Previous authors (3, 4, 5) have suggested pertinent correlation forms for liquid-liquid mass transfer to be sums or products of the Reynolds numbers and viscosity ratios in the two liquid phases and the molecular diffusivity of the transferring species. However, in this investigation the operating parameters varied were limited to the Reynolds number based on the stirrer tip speed and the cell geometry. The experimentation was conducted with a single solute and liquid pair, precluding any variation in the ratio of the liquid viscosities or the molecular diffusivity. Furthermore, the experimental apparatus did not permit the independent variation of the two liquid Reynolds numbers since both impellers were located on the same shaft. The mercury and water phase Reynolds numbers were always related by a multiplicative constant and consequently could not be distinguished in the correlations. The meaningful correlating groups possible in this investigation relate the mass transfer coefficient to a single Reynolds number, the cell size, and the liquid phase heights within the cell.

The principal operating parameter influencing the transfer of quinone in the water phase to the mercury-water interface was the Reynolds number. A product form correlation of the dimensionless mass transfer coefficient with the mercury-based Reynolds number yielded the following relationship:

$$\frac{KL}{\nu_m} = 2.58 \times 10^{-5} \, Re_m^{1.169 \pm 0.030} \qquad (17)$$

This equation had a correlation coefficient of 0.942 which indicates good agreement between the calculated and experimental mass transfer coefficients as shown in Fig. 8. This correlation form was expanded to include the geometric effects of cell size and liquid phase depth. Incorporating these effects, the correlation for the mass transfer coefficient was:

$$\frac{KL}{\nu_m} = 7.87 \times 10^{-5} \, Re_m^{1.087 \pm 0.031} \left(\frac{L}{H}\right)^{0.153 \pm 0.072} \left(\frac{L}{E}\right)^{0.306 \pm 0.088} \qquad (18)$$

The correlation coefficient for Eq. (18) was 0.953. This small increase was not considered significant and did not justify inclusion of the geometric factors in the mass transfer correlation.

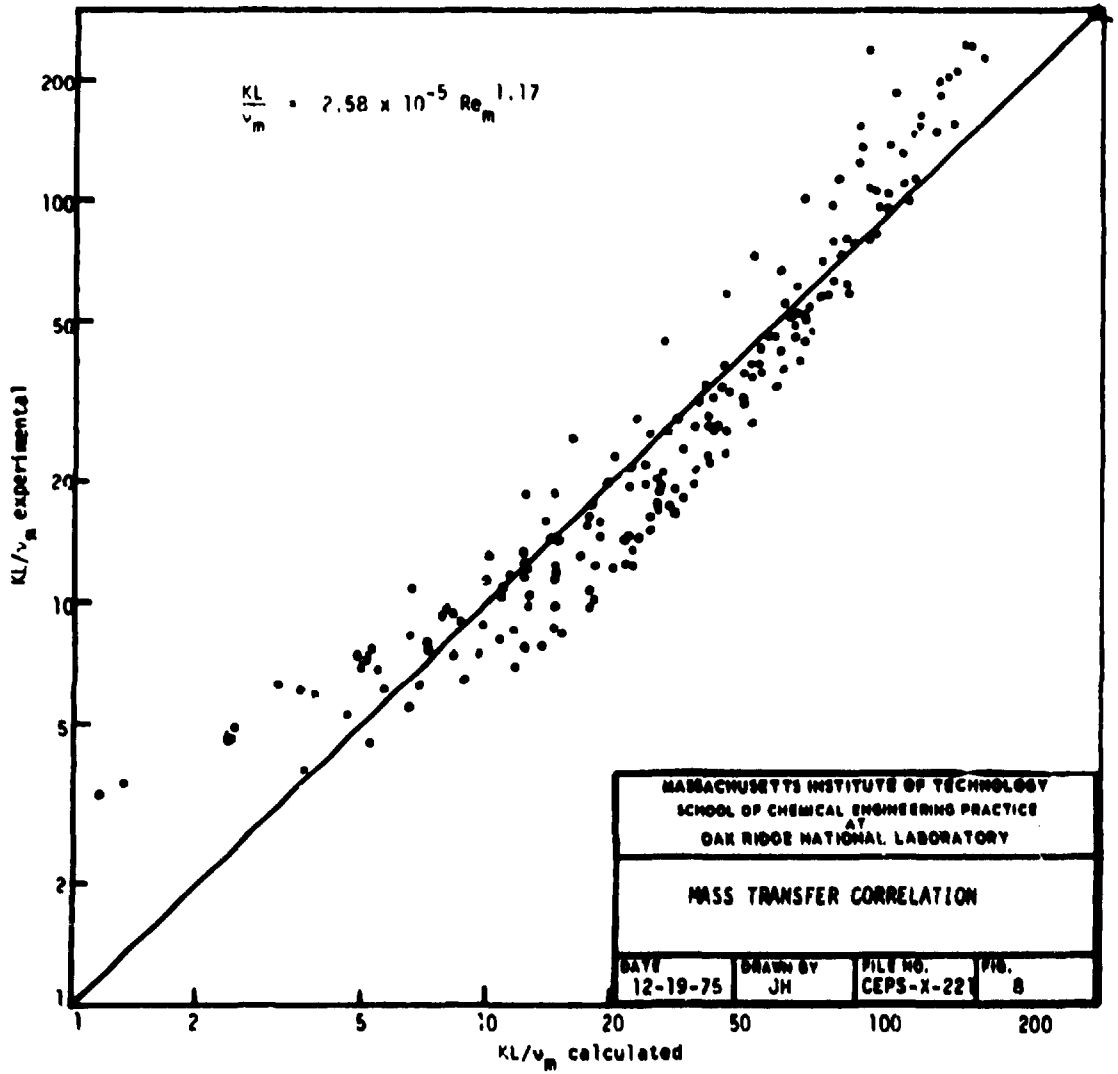
$\frac{KL}{\nu_m} = 2.58 \times 10^{-5} Re_m^{1.17}$
KL/ν_m experimental
KL/ν_m calculated
1
2
5
10
20
50
100
200
MASSACHUSETTS INSTITUTE OF TECHNOLOGY
SCHOOL OF CHEMICAL ENGINEERING PRACTICE
AT
OAK RIDGE NATIONAL LABORATORY
MASS TRANSFER CORRELATION
DATE 12-19-75
DRAWN BY JH
FILE NO. CEPS-X-22
FIG. 8

Inspection of the comparison shown in Fig. 8 illustrates that the mass transfer coefficient did not follow a simple power relationship with the Reynolds number. The logarithmic plot in Fig. 8 is slightly curved. This may be attributed to different flow or mixing regimes intrinsic to different Reynolds numbers. Possible controlling factors in these regions involve diffusion or free convection at low Reynolds numbers, eddy diffusion and transfer at intermediate Reynolds numbers, and vortexing at high Reynolds numbers. The diffusion and free convection were accounted for by extrapolation of Fig. 8 to low Reynolds numbers. The apparent mass transfer rate occurring at this condition was subtracted from all the experimentally measured transfer rates. The correlation obtained by this method was:

$$\frac{KL}{\nu_m} - 3 = 7.62 \times 10^{-7} \, Re_m^{1.447 \pm 0.030} \qquad (19)$$

having a correlation a correlation coefficient of 0.962. As shown in Fig. 9, this correlation eliminates the curvature apparent previously at the low Reynolds numbers. The exponent on the Reynolds number reflects the mass transfer dependency on the eddy diffusion alone, enabling a slightly better fit of the data at the larger Reynolds numbers. However, the wide deviation of the calculated values from the experimental observations implies a non-optimal value describing the diffusion contribution was selected, or that this term is a function of other operating parameters.

Several alternative correlation forms were attempted to describe the curvature at the higher Reynolds numbers. The mass transfer in the stirred cell was considered to occur in two distinct flow regions, and as such could be correlated by a linear combination of Reynolds numbers of the form:

$$\frac{KL}{\nu} = a + b \, Re^e + d \, Re^f \qquad (20)$$

The computerized correlation program available did not enable evaluation of both the exponents and coefficients in Eq. (20). Several techniques were applied in attempting to evaluate the exponents prior to correlation. The first technique assumed the two flow regimes to correspond to the individual water and mercury phases. Figure 7, which shows the mass transfer rate agitating one liquid phase only, can then be employed to determine the exponents in Eq. (20). A second technique involved correlating the mass transfer coefficient and Reynolds number by a simple power law equation over small intervals of Reynolds numbers. In this manner the variation in exponents from one regime to another may be isolated. Finally, an iterative search technique optimizing the values of the exponents was applied over the range of values suggested by the previous analysis. However, no linear combination of Reynolds numbers could be obtained which adequately described the measured mass transfer coefficient as had initially been expected.

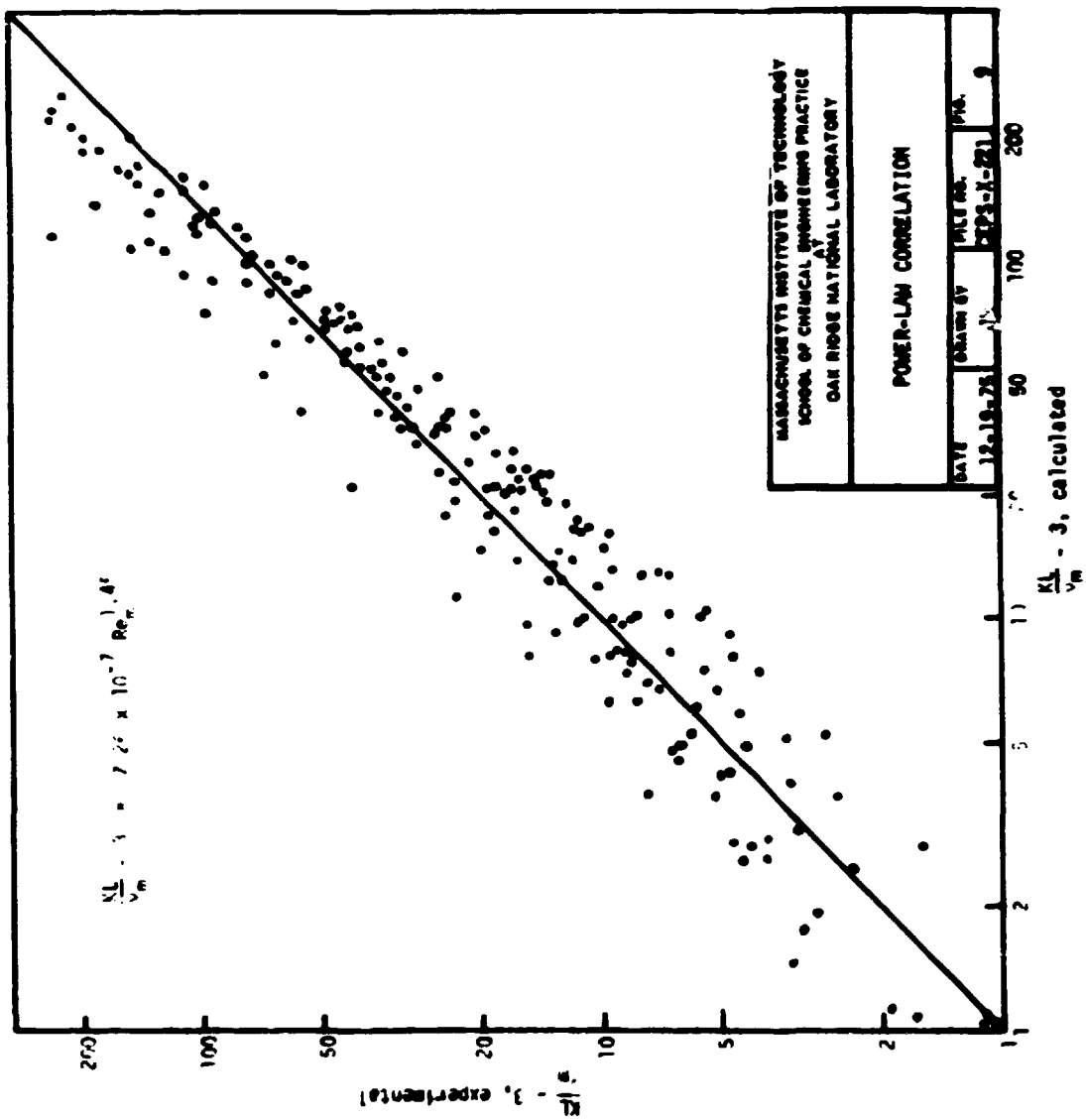
MASSACHUSETTS INSTITUTE OF TECHNOLOGY
SCHOOL OF CHEMICAL ENGINEERING PRACTICE
OAK RIDGE NATIONAL LABORATORY
POWER-LAW CORRELATION
DATE
DRAWN BY
FILE NO.
PG.
1
2
5
10
20
50
100
200
$\frac{kL}{\nu_m}$ - 3, calculated
$\frac{kL}{\nu_m}$ - 3, experimental

Examination of Figs. 7 and 8 suggested that the mass transfer coefficieint could be best represented by an exponential form of the Reynolds number. The best correlation of this form was:

$$\frac{KL}{\nu_m} = 0.0158\ Re_m^{0.561\pm0.053}\ \exp[Re_m(4.05 \pm 0.32) \times 10^{-6}] \qquad (21)$$

The correlation coefficient for Eq. (21) was 0.970. Furthermore, inspection of this correlation, shown on Fig. 10, indicates that much of the curvature existing previously at both low and high Reynolds numbers has been eliminated and a compaction of the calculated and observed mass transfer coefficients about the 45° line was noted. However, no physical model is presented which suggests this type of correlation. Significant difficulty was encountered in attempting to correlate the mass transfer coefficients corresponding to higher Reynolds numbers in Fig. 8, though these points may in fact represent experimental error. At high Reynolds numbers, substantial rippling and vortexing of the mercury surface was observed to occur, significantly increasing the interfacial surface area. The experimental and calculational techniques employed would register a higher mass transfer rate than was actually occurring. The curvature apparent in Fig. 7 may be a result of the mercury surface vortexing and not a transition to a different flow regime.

6. CONCLUSIONS

1. A direct dependence of mass transfer coefficients on agitator speed and blade length was found.

2. Phase volume has a very small influence on the mass transfer coefficient compared with the Reynolds number effect as exponents in Eq. (18) indicate.

3. Ferric chloride is not a satisfactory oxidizing agent for reacting with metals amalgamated with mercury due to its oxidation of the mercury.

4. Hydrochloric acid reacts with zinc too slowly for mass transfer experiments since the limiting step would be the reaction rate.

7. RECOMMENDATIONS

1. Experimentation on water-side mass transfer varying viscosity and density of solutions should be continued.

2. The time and expense of alternate experimental methods justify more development of the proposed procedure for mercury-side mass transfer

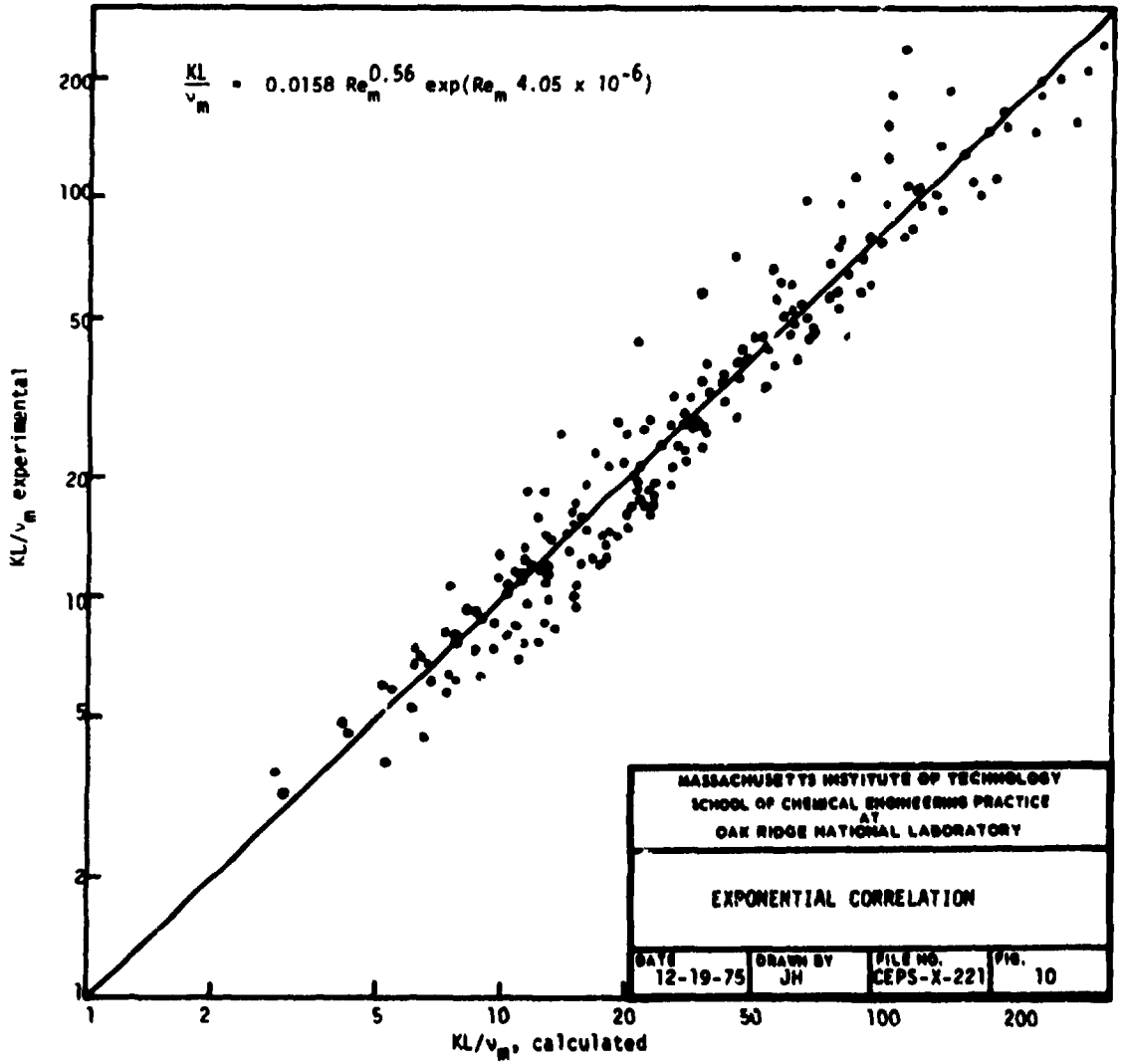
$\frac{KL}{\nu_m} = 0.0158\ Re_m^{0.56} \exp(Re_m\ 4.05 \times 10^{-6})$
KL/ν_m experimental
KL/ν_m, calculated
1
2
5
10
20
50
100
200
MASSACHUSETTS INSTITUTE OF TECHNOLOGY
SCHOOL OF CHEMICAL ENGINEERING PRACTICE
AT
OAK RIDGE NATIONAL LABORATORY
EXPONENTIAL CORRELATION
DATE 12-19-75
DRAWN BY JH
FILE NO. CEPS-X-221
FIG. 10

determination with further oxidizing agents and metals systems such as stannic ion/lead and hydrogen ion/magnesium.

8. ACKNOWLEDGMENTS

We would like to thank our consultants, J.R. Hightower and C.H. Brown, for their assistance throughout this project.

9. APPENDIX

9.1 Sample Calculations

Data were analyzed as shown below for Run J-28 (ORNL Databook A-7551-G). The mass transfer coefficient, K, was found applying Eq. (13). The diffusion current was found to be 121 mA. The interfacial area in all calculations was the cross-sectional area of the cell. Therefore,

$$K = \frac{I}{(Z)(F)(A)(C_B)}$$

$$= \frac{121 \times 10^{-3}\ A}{(2\ \frac{equiv}{mole})(96{,}487\ \frac{coul}{equiv})(1\ \frac{A\text{-}sec}{coul})(929\ cm^2)(2.0 \times 10^{-7}\ \frac{mole}{cm^3})}$$

$$= 3.38 \times 10^{-3}\ cm/sec$$

9.2 Location of Data

The original data are located in ORNL Databook A-7551-G, pp. 1-92. All calculations and the databook are on file at the MIT School of Chemical Engineering Practice, Bldg. 3001, ORNL.

9.3 Nomenclature

A interfacial area for mass transfer, cm^2

C concentration of reacting ion, $gmole/cm^3$

D diffusion coefficient, cm^2/sec

E width of cell, cm

F Faraday constant, coulombs/eq

H height of an individual pnase, cm

I polarization current, amp

J molar flux, $gmole/cm^2\text{-}sec$

K mass transfer coefficient, cm/sec

L tip-to-tip stirrer length, cm

N stirrer speed, rev/sec or rev/min

Q total molar flow rate, gmole/sec

R gas constant, joule/mole-°K

r distance from electrode surface, cm

Re Reynolds number, $L^2N\rho/\eta$, dimensionless

Sc Schmidt number, $\eta/\rho D$, dimensionless

T absolute temperature, °K

u mobility of ion

Z valence change of the transferring ion, eq/mole

η viscosity, gm/cm-sec

ν kinematic viscosity = η/ρ, cm^2/sec

ρ density, gm/cm^3

ϕ electric potential, v

Subscripts

1,2 phase being considered

b bulk phase

i interfacial

m mercury phase

a aqueous phase

9.4 References

1. "Handbook of Chemistry and Physics," 52nd ed., Chemical Rubber Co. (1971-72).

2. Hightower, J.R., "Engineering Development Studies for Molten-Salt Breeder Reactor Processing, No. 18," ORNL-TM-4698 (March 1975).

3. Lewis, J.B., "The Mechanism of Mass Transfer of Solutes Across Liquid-Liquid Interfaces," Chem. Eng. Sci., 3, 248 (1954).

4. Mayers, G.R.A., "The Correlation of Individual Film Coefficients of Mass Transfer in a Stirred Cell," Chem. Eng. Sci., 16, 69 (1961).

5. McManamey, W.J., "Molecular Diffusion and Liquid-Liquid Mass Transfer in Stirred Transfer Cells," Chem. Eng. Sci., 15, 251 (1961).